Biogeosciences Discuss., 11, 3271–3317, 2014
www.biogeosciences-discuss.net/11/3271/2014/
doi:10.5194/bgd-11-3271-2014

Biogeosciences Discussions
Open Access

Physical controls on CH_4 emissions from a newly flooded subtropical freshwater hydroelectric reservoir: Nam Theun 2

C. Deshmukh[1,2,*], D. Serça[1], C. Delon[1], R. Tardif[3], M. Demarty[4], C. Jarnot[1], Y. Meyerfeld[1], V. Chanudet[5], P. Guédant[3], W. Rode[3], S. Descloux[5], and F. Guérin[6,7]

[1]Laboratoire d'Aérologie – Université de Toulouse – CNRS UMR 5560; 14 Av. Edouard Belin, 31400, Toulouse, France
[2]TERI University, New Delhi, India
[3]Nam Theun 2 Power Company Limited (NTPC), Environment & Social Division – Water Quality and Biodiversity Dept. – Gnommalath Office, P.O. Box 5862, Vientiane, Laos
[4]Environnement Illimite, 1453 rue Saint Timothee, Montreal QC, Canada
[5]Electricité de France, Hydro Engineering Centre, Sustainable Development Dpt, Savoie Technolac, 73373 Le Bourget du Lac, France
[6]Université de Toulouse; UPS GET, 14 Avenue E. Belin, 31400 Toulouse, France
[7]IRD; UR 234, GET; 14 Avenue E. Belin, 31400, Toulouse, France
[*]now at: Nam Theun 2 Power Company Limited (NTPC), Environment & Social Division – Water Quality and Biodiversity Dept. – Gnommalath Office, P.O. Box 5862, Vientiane, Laos

Received: 3 February 2014 – Accepted: 17 February 2014 – Published: 26 February 2014

Correspondence to: D. Serça (dominique.serca@aero.obs-mip.fr)

Published by Copernicus Publications on behalf of the European Geosciences Union.

Abstract

In the present study, we measured CH_4 ebullition and diffusion with funnels and floating chambers in the footprint of an eddy-covariance system measuring CH_4 emissions at high frequency (30 mn) in the Nam Theun 2 Reservoir, a recently impounded (in 2008) subtropical hydroelectric reservoir located in Lao PDR, southeast Asia. The EC fluxes were very consistent with the sum of the two terms measured independently (diffusive fluxes + ebullition = EC fluxes), indicating that the EC system picked-up both diffusive fluxes and ebullition from the reservoir. The EC system permitted to evidence a diurnal bimodal pattern of CH_4 emissions anti-correlated with atmospheric pressure. During daytime, a large atmospheric pressure drop triggers CH_4 ebullition (up to 100 $mmol\,m^{-2}\,d^{-1}$) whereas at night, a more moderate peak of CH_4 emission was recorded. As a consequence, fluxes during daytime were twice higher than during nighttime.

A total of 4811 measurements of CH_4 ebullition with submerged funnels at a weekly/fortnightly frequency were performed. The data set covers a water depth ranging from 0.4 to 16 m, and all types of flooded ecosystems. This dataset allowed to determine that ebullition depends mostly on water level change among many other variables tested. On average, ebullition was $8.5 \pm 10.5\,mmol\,m^{-2}\,d^{-1}$ (10–90 percentile range: 0.03–21.5 $mmol\,m^{-2}\,d^{-1}$) and ranged from 0–201.7 $mmol\,m^{-2}\,d^{-1}$. An artificial neural network model could explain up to 45 % of variability of ebullition using total static pressure (sum of hydrostatic and atmospheric pressure), variations in the water level and atmospheric pressure, and bottom temperature as inputs. This model allowed extrapolation of CH_4 ebullition at the reservoir scale and performing gap-filling over four years. Our results clearly showed a very high seasonality: 50 % of the yearly CH_4 ebullition occurs within four months of the warm dry season. Overall, ebullition contributed 60–80 % of total emissions from the surface of the reservoir (disregarding downstream emissions) suggesting that ebullition is a major pathway in young hydroelectric reservoirs in the tropics.

BGD
11, 3271–3317, 2014

1 Introduction

Atmospheric methane (CH_4) mixing ratio has recently reached up to 1875 ppb, which is 162 % higher than the pre-industrial value (IPCC, 2013), and is the highest mixing ratio ever reported (Dlugokencky et al., 2009). Currently, CH_4 is directly and indirectly responsible for 43 % of the anthropogenic radiative forcing (IPCC, 2013). Inland waters (wetlands, lakes, reservoirs, rivers and ponds) are the main source of CH_4 on Earth (Bastviken et al., 2011; IPCC, 2013). All together, the CH_4 emissions from inland waters would represent 40 % of total CH_4 emissions and 75 % of natural CH_4 emissions (IPCC, 2013) and correspond to 50 % of the carbon terrestrial sink (Bastviken et al., 2011). The order of magnitude of CH_4 emissions from inland waters is probably conservative (Bastviken et al., 2011). However, these estimates are based on dataset characterized by little temporal and spatial resolution (Bastviken et al., 2004; Barros et al., 2011) although a few studies evidenced strong diurnal variations (Bastviken et al., 2010; Sahlée et al., 2014), seasonal variability (e.g., Abril et al., 2005), transient extreme emissions (e.g., Varadharajan and Hemond, 2012; Sahlée et al., 2014) and strong spatial variations (e.g., Del Sontro et al., 2011; Morrissey and Livingstone, 2012). Therefore, it is possible that hot moments and hot spots of emissions were overlooked leading to a potential underestimation of emissions at the global scale.

Among the different known CH_4 pathways to the atmosphere, diffusive fluxes and ebullition have the most studied ones in natural lakes and anthropogenic water bodies (i.e., hydroelectric reservoirs, farm ponds ...). Ebullition of CH_4 corresponds to vertical transfer of CH_4 from the sediment to the atmosphere with little physical and biological interactions within a shallow (< 20 m) water column (McGinnis et al., 2006). Methane is produced in anoxic condition in the sediments or the flooded soils during the mineralization of organic matter. CH_4 bubbles can develop if CH_4 concentration in the interstitial water becomes higher than the maximum solubility of this gas in water. Bubbling fluxes mainly occur in shallow part of lakes and hydroelectric reservoirs (Abril et al., 2005; Bastviken et al., 2004; Galy-Lacaux et al., 1997; Keller and Stallard, 1994)

BGD
11, 3271–3317, 2014

where the hydrostatic pressure is low. The release of the bubbles is triggered by atmospheric pressure variations (Casper et al., 2000; Eugster et al., 2011; Fechner-Levy and Hemond, 1996; Mattson and Likens, 1990; Tokida et al., 2005; Wik et al., 2013), variations in water current velocity (Martens and Klump, 1980; Chanton et al., 1989; Scranton et al., 1993), shear stress at the sediment surface (Joyce and Jewell, 2003), variation of the water level above the sediment (e.g., Boles et al., 2001; Chanton et al., 1989; Engle and Melack, 2000; Martens and Klump, 1980; Smith et al., 2000), increase of temperature that makes the CH4 solubility decrease (Chanton and Martens, 1988) and strong wind events (Keller and Stallard, 1994). Ebullition is episodic, which make it difficult to accurately quantify. Bubbling fluxes are probably always underestimated (Bastviken et al., 2011; Glaser et al., 2004; Wik et al., 2013), thus they must be determined as frequently as possible. In most of the ecosystems where it was determined by discrete sampling with funnels, ebullition was shown to dominate diffusive fluxes (Bastviken et al., 2011).

Diffusive CH_4 fluxes at the air–water interface depend on the concentration gradient between the surface water and the atmosphere. They are usually estimated either by calculations or by floating chambers (FC). The calculation by the thin boundary layer (TBL) model (Liss and Slater, 1974) is based on the concentration gradient between the water surface and the atmosphere and a gas transfer velocity. In the literature, the gas transfer velocity is related for instance to wind speed (e.g. Borges et al., 2004; Cole et Caraco, 1998; Frost and Upstill-Goddard, 2002; Guérin et al., 2007), rainfall rates (Ho et al., 1997; Guérin et al., 2007), buoyancy fluxes (McIntyre et al., 2011) or water current velocity (e.g., Borges et al., 2004). The limit of this approach is that these relationships are site specific (Borges et al., 2004; Kremer et al., 2003b), leading to uncertainties when applied without precaution. Fluxes can also be obtained on site by the use of FCs. This technique is frequently criticized because FCs are supposed to either artificially increase turbulence, specially at low wind speed (Matthews et al., 2003; Vachon et al., 2010), or decrease turbulence by isolating the surface water from the wind friction (Liss and Merlivat, 1986). Nevertheless, FCs were shown to give results in

BGD
11, 3271–3317, 2014

fair agreement compared to other methods in some aquatic ecosystems (Kremer et al., 2003a; Guérin et al., 2007). Whereas in some other ones where CH_4 ebullition is very intense, FC integrates both diffusion and ebullition (Bastviken et al., 2010). In this latter case, diffusion contribution to total emission cannot be measured by FC except with the adaptation of a bubble shields as developed by Bastviken et al. (2010).

Eddy covariance (EC) measurements of CH_4 emissions are becoming feasible with suitable fast-response sensors now available on the market (e.g. Eugster and Plüss, 2010; McDermitt et al., 2010). It is therefore realistic to quantify CH_4 emissions with EC technique at a scale representative of a wide range of ecosystems (typically hectares). Still, very few EC field deployments have been conducted so far to determine CH_4 emissions, whether in freshwaters lakes (Schubert et al., 2012) or man-made reservoirs (e.g. Eugster et al., 2011). EC was show to be able to capture both diffusive flux and ebullition (Eugster et al., 2011), but with no discrimination between the two pathways. However, the deployment of EC that captures continuously the emissions with a short time resolution (e.g., 30 min), over long periods (day to year), and large areas (typically hectares) in combination with classical discrete sampling and calculations for diffusion and ebullition should provide information on the short term and daily variability of CH_4 emissions by its different pathways.

In the present study, CH_4 emission was measured with EC, FC and funnels and calculated by TBL at the Nam Theun 2 (NT2) Reservoir in Lao PDR, Southeast Asia. First, the different methods were compared according to the CH_4 pathways they capture. Once all methods were validated, high frequency measurements over diurnal cycles at different seasons obtained with EC were used for the determination of the physical controls on CH_4 emissions and pathways on a daily basis. Based on a weekly monitoring of ebullition during one and half year, we examined its controlling factors in order to estimate ebullition at the entire reservoir scale. This was finally achieved with an artificial neural network approach which allowed us to simulate over a four-year period the ebullition for the entire reservoir from the controlling factors.

BGD
11, 3271–3317, 2014

2 Site description

The Nam Theun 2 (NT2) hydroelectric reservoir (17°59′49″ N, 104°57′08″ E) was built on the Nam Theun River, in the subtropical region of Lao People's Democratic Republic (Lao PDR). Filling of the reservoir began in April 2008, and the full water level of the reservoir (538 m msl) was reached for the first time in October 2009. At maximal water level, the reservoir floods a 489 km^2 dendritically shaped area which was mainly covered by dense and medium forests (44.7 %), light and degraded forests (36.4 %), agricultural lands (11 %), with the remaining made up by swamps and rivers (Descloux et al., 2011).

The study site is under a subtropical monsoon climate. The classical meteorological years can be separated into three seasons: warm wet season (WW) from mid-June to mid-October, cool dry season (CD) from mid-October to mid-February, and warm dry season (WD) from mid-February to mid-June (NTPC, 2005). Since the water inputs to the NT2 Reservoir are directly related to rainfall, filling of the reservoir typically occurs during the WW season when study area receives 80 % of annual rainfall (NTPC, 2005). Since the beginning of power plant operation (March 2010), the reservoir water level had varied seasonally, and achieved its maxima and minima respectively during the WW season, and by the end of the WD season. During the period covered by this study, the reservoir water level varied seasonally by up to 9.5 m, which corresponded to a variation in the reservoir water surface from 168 to 489 km^2. With an annual average depth of 7.8 m, NT2 Reservoir falls among the shallow reservoir category.

3 Methods

3.1 Sampling strategy

The EC system was deployed in an open water area (17°41.56′ N, 105°15.36′ E) chosen to offer a smooth fetch in all directions. At this location, fetch varied from about 1 km

BGD
11, 3271–3317, 2014

(northeast), to more than 10 km (northwest). Eddy covariance was deployed four times to study the CH_4 emission during a variety of meteorological and environmental conditions. Two deployments (3 days in May 2009 and 5 days in June 2011) were performed during the transition between the WD season and the WW season. Average water depth was ~ 10 and ~ 1.5 m in May 2009 and June 2011, respectively. The two other field campaigns (14 days in March 2010 and 5 days in March 2011) occurred during the transition between the CD and the WD seasons. Average water depth was ~ 10.5 m and ~ 6.5 m in March 2010 and March 2011, respectively. During the May 2009 campaign, reservoir water level was increasing with a mean rate of 1.0 cm d^{-1}, whereas, the other three campaigns were performed during falling reservoir water level with mean rates of −4.5, −4.6 and −6.9 cm d^{-1} respectively for March 2010, March 2011 and June 2011. Statistical details of the different meteorological parameters for four EC deployments are summarized in Table S3.

During each EC deployment, independent measurements of the diffusive and ebullitive fluxes were performed in the footprint of the EC set up with FC and funnels, respectively. Each FC measurement was done together with surface water sampling devoted to the determination of the CH_4 concentration. Note that in March 2010, funnel measurements could not have been performed around the EC set up.

Additional ebullition of CH_4 measurements were performed with funnels during five field campaigns covering different seasons, from May 2009 to June 2011, and all along a weekly monitoring from March 2012 to August 2013. During this later monitoring, spatial variation was explored through measurements at sites representative of the different types of flooded ecosystems (dense and medium forests, light and degraded forest and agricultural lands, Descloux et al., 2011), and for different depths (from 0.4 to 16 m) at each sampling site.

3.2 Instrumentation of EC system

The basic EC instrumentation included a 3-D sonic anemometer (Windmaster Pro, Gill Instruments, Lymington Hampshire, UK, in May 2009 and March 2010 and a CSAT-3,

BGD
11, 3271–3317, 2014

Campbell Scientific, Logan, UT, USA, in March 2011 and June 2011), and a closed-path fast methane analyzer (DLT-100 FMA, Los Gatos Research, CA, USA). Data acquisition was carried out at 10 Hz with a Campbell datalogger (CR3000 Micrologger®, Campbell Scientific).

Air was carried to the DLT-100 through a 6 m long tube (Synflex-1300 tubing, Eaton Performance Plastics, Cleveland) with an internal diameter of 8 mm. The tube inlet, protected by a plastic funnel to avoid entry of rainwater, was mounted 0.20 m behind the sonic anemometer sensors. An internal 2 µm Swagelok filter was used to protect the sampling cell from the dust, aerosols, insects and droplets. High frequency sampling of air was obtained by the use of a dry vacuum scroll pump (XDS35i, BOC Edwards, Crawly, UK) providing a flow rate of 26 $L\,mn^{-1}$. Due to the remote location of our study site, a 5 kVA generator running on the gasoline was used for the power supply of the whole EC instrumentation. Possible contaminations of the atmospheric CH_4 concentration measurements from the generator were checked using the wind direction and a footprint model (Kljun et al., 2004).

During each EC deployment, wind speed, wind direction, atmospheric pressure, atmospheric temperature, relative humidity and rainfall were measured using a meteorological station (Weather Transmitter Model WXT510, Helsinki, Finland). A radiometer (CNR-1, Kipp & Zonen, Delft, the Netherlands) was used to measure upcoming and outgoing short and longwave radiations. The temperature of surface water was measured at 20 cm depth using a thermister (Pt100 sensor) coupled to the datalogger.

3.2.1 Data processing

The 10 Hz raw were processed using the EdiRe software (Clement, 1999; University of Edinburgh) for the following steps: (1) spike detection using a standard de-spiking algorithm whereby wind vector and scalars values greater than three times the standard deviation are removed, (2) lag correction and tube attenuation relevant to the closed path DLT-100 gas analyzer, (3) coordinate rotation using the planar fit method, and (4)

BGD
11, 3271–3317, 2014

high frequency correction factors to take into account the loss at high frequency due to insufficient sampling rate.

Differences among the deployments specific variables i.e. sensor separation distance and instrument placement were considered while processing the data. The EC fluxes of CH_4 were calculated as covariance between the scalars and vertical wind speed fluctuations according to commonly accepted procedures (Aubinet et al., 2001). Fluxes were considered positive if they were directed from the water surface toward the atmosphere, and negative otherwise.

3.2.2 EC data quality control

Fluxes were accepted or rejected according to the following criterion. First, a nonstationarity criterion was applied according to Foken and Wichura (1996). Fluxes were considered stationary and therefore accepted only if the difference between the mean covariance of sub records (5 mn) and the covariance of the full period (30 mn) was less than 30 %. Second, a flux was rejected if its intermittency rose above one (Mahrt et al., 1998). Third, for vertical wind component, the skewness and kurtosis were used to stay within the range of (−2, 2) and (1, 8), respectively (Vickers and Mahrt, 1997). Fourth, the momentum flux, $\overline{u'w'}$, was required to be negative implying a downward directed momentum flux. In addition, fluxes were rejected when the wind was coming from the power generator unit according to the footprint model of Kljun et al. (2004). For footprint analysis, since the roughness length value was unknown, we considered a value of 0.0002 m, as reported for terrain without obstacle (WMO, 2008). According to the model, the footprint was different in extension and prevalent wind directions among the different field campaigns. The smallest footprint area was observed during the March 2010 campaign, and the biggest for June 2011, with the greatest values rarely exceeding 500 m. The analysis confirmed that (1) surrounding terrestrial ecosystems were always outside the footprint, (2) only 2 % of the fluxes were rejected because wind was coming from the power generator, and (3) all FC and funnels measurements were conducted within the EC footprint area.

BGD
11, 3271–3317, 2014

As mentioned by Eugster et al. (2011), the minimum threshold for friction velocity cannot apply as a good criterion for flux rejection since turbulence generated due to heat loss from the water column can contribute significantly to the emissions to the atmosphere (Eugster et al., 2003, 2011; MacIntyre et al., 2002, 2010). In addition, the criteria on atmospheric concentration formulated by Vickers and Mahrt (1997) for CO_2 over terrestrial ecosystems do not apply for CH_4 over an aquatic ecosystem since emissions could be sporadic due to potential CH_4 burst linked to ebullition (Eugster et al., 2011).

Quality control criteria applied all together resulted in the acceptance of 57 % of the flux data, with acceptance rates slightly more important during daytime (59 %), than nighttime (52 %) periods.

3.3 Diffusive fluxes

3.3.1 Measurement by floating chamber (FC)

Diffusive flux measurements around the EC site were performed with two circular floating chambers (FC_{GC}), (surface area = 0.15 m^2; volume = 24.6 L) following the same design as in Guérin et al. (2007). Moreover, FCs were covered with a reflective surface to limit warming inside the chamber during measurements. Within 45 mn, four air samples with duplicates were collected with a syringe from the chambers at 15 mn interval. Air samples were collected in 10-ml glass vials which contained 6 M NaCl solution capped with butyl stoppers and aluminum seals as described in Angel and Conrad (2009). All samples were analyzed within 48 h by GC. Diffusive fluxes (D_{GC}) were calculated from the slope of the linear regression of gas concentration in the chamber vs. time. The fluxes were accepted when the correlation coefficient (r^2) of the linear regression was higher than 0.80. Linearity of the correlation coefficient can be affected by ebullition along the diffusive flux determination. For flux measurements with correlation coefficient lower than 0.8, a "total" flux, including diffusion and ebullition without distinction (and subsequently noted DE_{GC}, see Sect. 4.1) was calculated.

BGD
11, 3271–3317, 2014

In March 2011, a floating chamber (surface area = 0.16 m^2; volume = 17.6 L) connected to a Picarro® CH_4 analyzer (FC_{GA}) was also deployed to measure diffusive fluxes (D_{GA}). The calculation and rejection procedures are identical to the ones described above for D_{GC}.

3.3.2 Estimate from surface CH_4 concentrations

Surface water samples for CH_4 concentration were taken with a surface water sampler following the procedure by Abril et al. (2007). Water samples were stored in 60 mL glass vials, capped with butyl stoppers, sealed with aluminum crimps and poisoned until analysis (Guérin and Abril, 2007). Before Gas-Chromatography (GC) analysis for CH_4 concentration, a N_2 headspace was created and the vials were vigorously shaken to ensure an equilibration between liquid and gas phases (i.e. Guérin and Abril, 2007). The specific gas solubility for CH_4 (Yamamoto et al., 1976) as a function of temperature was used for calculation of CH_4 concentrations dissolved in water.

The surface CH_4 concentrations were used together with atmospheric concentrations measured on site in order to calculate diffusive fluxes with Eq. (1):

$$D_{TBL} = k_T \cdot C_w - C_a \quad (1)$$

where D_{TBL} is the diffusive flux at water–air interface, k_T the gas transfer velocity for a given temperature (T), C_w the CH_4 concentration in surface water, and C_a the CH_4 concentration in the overlying atmosphere. The k_T values were computed with the following Eq.:

$$k_T = k_{600} \cdot (600/Sc_T)^n \quad (2)$$

with Sc_T, the Schmidt number of CH_4 at a given temperature (T) (Wanninkhof, 1992); n, a number that is either 2/3 for low wind speed (< 3.7 $m\,s^{-1}$) or 0.5 for higher wind speed (Jahne et al., 1987).

BGD
11, 3271–3317, 2014

Since many of the diffusive fluxes measured by FC were contaminated by ebullition of CH_4, no relationship of k_{600} with any environmental variables such as wind speed or rainfall rates was found in the database of accepted fluxes. The D_{TBL} values were then calculated according to the formulation of k_{600} vs. wind speed from MacIntyre et al. (2010) and Guérin et al. (2007), the average of both formulations being used in the manuscript. These formulations were chosen because MacIntyre et al. (2010) includes the effect of buoyancy fluxes in the gas transfer velocity, and because Guérin et al. (2007) is one of the very few available for tropical hydroelectric reservoirs.

3.4 Ebullition of CH_4

Clusters of five to ten funnels (diameter = 26 cm) attached to each other at 1 m distance were assembled. Three to six clusters were positioned below the water surface at locations with different water depths around the same site (within 10–30 m). The funnels remained on sites for 24 or 48 h. Accumulated gas volumes were collected manually using a 60 mL syringe and stored in glass vials which contained 6 M NaCl solution. All gas samples were analyzed for CH_4 within 48 h by GC. CH_4 bubble concentrations were multiplied by the volume of accumulated bubbles over the deployment period to determine CH_4 ebullition fluxes (E_{FUN}). The ebullition was also determined from the FC_{GA} measurements in March 2011. The sudden increase of the CH_4 concentrations in the FC_{GA} were attributed to bubbles, and subsequent ebullition fluxes E_{GA} were calculated on the deployment time of FC measurement (typically 5 to 20 mn).

3.5 Gas chromatography

Analysis of CH_4 concentration was performed by gas chromatography (SRI® 8610C gas chromatograph, Torrance, CA, USA) equipped with a flame ionization detector (FID). A subsample of 0.5 mL from the headspace of water sample vials and 1 mL of air from flux sample vials were injected. Commercial gas standards (2, 10 and 100 ppmv, Air Liquid "crystal" standards and mixture of N_2 with 100 % CH_4) were injected after

BGD
11, 3271–3317, 2014

analysis of every 10 samples for calibration. Duplicate injection of samples showed repeatability better than 5 %.

3.6 Artificial Neural Network

An Artificial Neural Network (ANN) was used to find the best non-linear regression between ebullition fluxes and relevant environmental variables. The ANN used in this study is the multi layer perceptron (MLP). The database of raw data was composed of 4811 individual ebullition fluxes. Fluxes from a given station measured the same day and at the same depth were averaged, leading to a final database for ANN composed of 510 lines, and 4 columns (one output, and 3 inputs, see discussion paragraph for the choice of the inputs). The dataset used by the MLP is separated in two pools, the training set (330 lines) and the validation set (180 lines). During the training process, a set of optimal weights is determined, that is subsequently applied to the validation set.

The ANN used in this study is based on a commercial version of the Neuro One 5.0© software, (Netral, Issy les Moulineaux, France). Some details concerning this specific study are given in this paragraph, and in the Supplement section. The whole description of the methodology is detailed in Delon et al. (2007). The architecture of the MPL (deduced from the Vapnik–Chervenenkis theory; Vapnik, 1995) is composed of 3 hidden neurons. All inputs and output are normalized and centered in order to avoid artifact in the training process. After normalization, the data have the same order of magnitude. The network is used in a static version where the lines of the database are independent of each other.

Weight values associated to each input are modified a 100 times (optimization process). Ten initializations (10 series of different sets of weights) are tested for each model. This configuration (100 modifications of weights, 10 models) is tested several times, in order to avoid a local minimum solution.

The best algorithm within the 10 launched is chosen, by assessing the following criteria: (1) The lowest generalization cost is chosen, (2) Root Mean Square Error (RMSE)

BGD
11, 3271–3317, 2014

of the training set has to be close to the RMSE of the validation set (23.09 and 23.83 in our case), and (3) results giving negative fluxes are discarded. Learning (training) cost is 6.79, validation cost is 6.9, generalization cost is 7.47, and homogeneity is 0.93, which are considered as good enough criteria for choosing the equation. The equation, coefficients and weights necessary to calculate the ebullition flux are listed in the Supplement, and in Tables S1 and S2.

3.7 Statistical analysis

The methodological, spatial and temporal differences in the CH_4 emissions were explored. Differences among groups of data were examined using either *t* test or Analysis of Variance (ANOVA) in GraphPad Prism (GraphPad Software, Inc., v5.04). Choice of the parametric and non-parametric test (Mann Whitney test or Kruskal–Wallis test compares median values) was dependent on normal and non-normal behavior of the data sets. The spatial differences of ebullition fluxes were explored on three clusters: (1) dense forest which includes dense and medium forest, (2) degraded forest which includes light and degraded forest and, (3) agricultural lands. The effect of depth on ebullition was also tested according to the following three depth ranges: shallow zones (0.4–3 m), intermediate (3–6 m) and deep (6–16 m). We examined the temporal variability in the fluxes on a seasonal basis. All statistical tests used a significance level of 5 %. The distributions of the volume of gas emitted by ebullition, CH_4 bubble concentration and flux were characterized using the Anderson–Darling Goodness of fit in EasyFit 5.5 trial version. A multi linear regression (MLR) was used to find the linear relationship between ebullition fluxes and other environmental variables. The MLR used in this study was based on the SPSS 15.0 for Windows.

3.8 Reservoir water temperature, meteorological and hydrological variables

The temperature at the bottom of the reservoir have been monitored on the fortnightly basis at nine sampling stations in the reservoir, from January 2009 to date. Meteoro-

BGD
11, 3271–3317, 2014

logical (wind speed, atmospheric pressure, atmospheric temperature, relative humidity, wind direction and net radiation) and hydrological data (rainfall and reservoir water level) were obtained from the monitoring conducted by Electricité de France and Nam Theun 2 Power Company Ltd. (NTPC).

4 Results and discussion

4.1 Assessment of CH_4 emissions at the reservoir surface by different methods

The effectiveness of four methods to measure CH_4 emissions at the water–air interface were explored during four field campaigns at NT2 (Table 1). Using these methods, different emission terms were estimated: (1) FC and TBL for diffusion at the air–water interface, (2) funnel and FC_{GA} for ebullition, and (3) EC and FC_{GC} techniques for total emissions (diffusion plus ebullition). Whatever the methods applied and the emissions pathways, the reservoir emitted CH_4 to the atmosphere during the studied period (Table 1). All methods were only used simultaneously in March 2011 (Fig. 1).

Only 30 % of the diffusive fluxes measured by the FC_{GC} fulfilled the acceptance criterion during the four field campaigns. No fluxes were accepted in March 2011, when the water level of the reservoir was decreasing, and only 5 % in June 2011, when the water level was its lowest. In March 2011, 48 % of the diffusive fluxes measured by FG_{GA} were accepted. The comparison of the acceptance percentages in March 2011 evidences that short-term deployment of chambers (5 mn for FC_{GA} vs. 45 mn for FC_{GC}) limits the risk of a contamination of the measurement by ebullition. Overall, the average D_{GC} is $1.1 \pm 0.7\,\mathrm{mmol\,m^{-2}\,d^{-1}}$ (0.2 to $2.4\,\mathrm{mmol\,m^{-2}\,d^{-1}}$, Table 1), which is comparable with the average D_{TBL} of $1.4 \pm 2.0\,\mathrm{mmol\,m^{-2}\,d^{-1}}$ (0.07–$14.8\,\mathrm{mmol\,m^{-2}\,d^{-1}}$, Table 1). for the four field campaigns. For all campaigns except June 2011 (only one validated measurement), the D_{TBL} calculations were not significant different from the diffusive fluxes measured with FC (t test, $p < 0.05$; details in Table 2). Combining all diffusive

BGD
11, 3271–3317, 2014

fluxes obtained by different approaches, our results showed that there is no seasonal variation for the diffusive fluxes measured (t test, $p < 0.05$; details in Table 2).

The ebullition of CH_4 was measured with funnels (E_{FUN}) in May 2009, March and June 2011, and using a FC_{GA} (E_{GA}) in March 2011 (Tables 1, and Fig. 1b). One of the major differences between these two methods is the duration of the measurement. E_{FUN} measurements were performed over 24 to 48 h, whereas E_{GA} measurements were conducted during only 5 to 20 mn. In June 2011, E_{FUN} (28.0 ± 11.0 mmol m^{-2} d^{-1}) were almost twentyfold and sevenfold higher than E_{FUN} in May 2009 and March 2011, respectively (Table 1). In March 2011, E_{FUN}varied by 2 orders of magnitude from 0.2 to 21.7 mmol m^{-2} d^{-1} with an average of 4.2 ± 3.6 mmol m^{-2} d^{-1}, which is not statistically different from E_{GA} during the same field campaign (4.6 ± 7.1 mmol m^{-2} d^{-1}, Tables 1 and 2). It has to be noted that ebullition was observed in around 50 % of FC_{GA} deployment.

The individual 30 mn DE_{EC} fluxes varied by four orders of magnitude during all EC deployments (Table 1). On average, DE_{EC} fluxes varied oppositely with the water depth, with the highest mean flux (29 ± 16 mmol m^{-2} d^{-1}) in June 2011 for the shallowest water depth (~ 1.5 m) (Table 1, and Fig. 2). Figures 1c and 2 show CH_4 fluxes measured using floating chamber which were affected by bubble (DE_{GC}). Altogether, DE_{GC} varied between 0.02 to 132 mmol m^{-2} d^{-1} (Table 1). In some cases, DE_{GC} was significantly different compare to DE_{EC} (Table 2, Fig. 2). This suggests that such sporadic measurements of high fluxes due to bubbles in the FC can lead to an over-estimation of the CH_4 emissions.

We compared continuous DE_{EC} with the sum of the discrete sampling of diffusive (D_{GC}, D_{GA} and D_{TBL}) and ebullitive fluxes (E_{FUN} and E_{GA}) for three field campaigns (May 2009, March and June 2011) among four since no ebullition measurements were done within the footprint in March 2010. Statistical analysis of the March and June 2011 data shows that DE_{EC} and the sum of diffusive fluxes and ebullition are similar (Table 2 and Fig. 2). This confirms that the EC system is able to pick-up both diffusive fluxes and ebullition from the reservoir as already shown by Schubert et al. (2012). Statistical analysis of May 2009 data shows that DE_{EC} are significantly different ($p = 0.1075$,

BGD
11, 3271–3317, 2014

Table 2) with the sum of the diffusion and ebullition discrete sampling. This difference might partly be due to the insufficient effort on funnels deployment during that campaign (only 9 individual funnels measurements within the footprint, Tables 1 and 2).

The sum of independent estimates of diffusive fluxes (D_{TBL}, D_{GC}, D_{GA}) and ebullition (E_{FUN} and E_{GA}) determined on less than a m^2 is in general in very good agreement with total emissions determined from EC over thousands of m^2. But, in a handful occasions, DE_{GC} and DE_{EC} exceed D_{TBL}, D_{GC}, D_{GA} by a factor up to 100 (Fig. 1c). If these observed differences were due to diffusion, the final CH_4 concentrations measured in the FC_{GC} could only be explained by diffusive fluxes up to 132 $mmol\,m^{-2}\,d^{-1}$. According to observed surface CH_4 concentrations for these extreme fluxes (from 0.1 to 12.9 $\mu mol\,L^{-1}$ this would correspond to very high gas transfer velocities (up to 225 $cm\,h^{-1}$). Such values of gas transfer velocities were never observed even during hurricane over the ocean (McNeil and D'Asaro, 2007). Since no such conditions occurred during the period covered by this study, the differences can only be explained by ebullition. The estimate of ebullition from 15 to 60 funnels covering a cumulated surface smaller than a m^2 during twenty-four hours was always very similar to the estimates from 30 mn-EC fluxes determined over large surfaces, whereas large discrepancies were observed when measured over a short period of time and a small surface (i.e. from sharp increase of CH_4 concentration detected in FC). This reveals very strong spatial and temporal heterogeneities of the ebullition process. Because ebullition is highly sporadic and occurs during very short period of time (Varadharajan and Hemond, 2012), its measurement by FC over short period of time and small surface area might lead to an over-estimation of this emission pathway if hot spots and hot moments are captured during the deployment of the chamber. Globally the EC measurements are ideal for capturing the large spatial and temporal variability of total CH_4 fluxes at the surface of aquatic ecosystems prone to ebullition. However, the discrimination of diffusive fluxes and ebullition requires the deployment of either FC to obtain the diffusive emissions or the deployment of funnels to obtain the ebullition. The use of recent techniques like the equilibrator technique (Abril et al., 2006) and subsequent

BGD
11, 3271–3317, 2014

TBL calculations for diffusive fluxes, or hydroacoustic measurement which is capable to capture the hot spots of ebullition (DelSontro et al., 2011) combined to the EC might allow the identification of those hot moments and their controlling factors.

Based on the results of the four campaigns, ebullition contributes between 57 and 93 % of the total CH_4 emissions from the EC footprint (Table 1 and Fig. 2). As already mentioned in some recent publications (Bastviken et al., 2004, 2010; DelSontro et al., 2010, 2011; Schubert et al., 2012), ebullition is a major CH_4 pathways that is often neglected in aquatic ecosystems, specially in the tropics and subtropics where the high temperature triggers ebullition by both enhancing CH_4 production in the sediments (Duc et al., 2010), and decreasing CH_4 solubility in the water column (Yamamoto et al., 1976).

4.2 Total CH_4 emissions (DE_{EC}) vs. hydrostatic pressure

The analysis of the four field campaigns time series from the EC system (Fig. S1) evidences that DE_{EC} were not controlled by the wind speed and the buoyancy fluxes (Fig. S2). As these parameters are known controlling factors of the diffusive fluxes (e.g., Guérin et al., 2007; McIntyre et al., 2010), it indirectly confirms that ebullition dominates the total emissions at the surface of the NT2 Reservoir, as shown in the previous section.

Daily DE_{EC} were plotted against the daily (1) water depth and (2) change in the water depth ($cm\,d^{-1}$), and (3) specific water level change (water level change normalized by the average water depth) (Fig. 3). DE_{EC} is negatively correlated to the water depth ($p < 0.0001$, Fig. 3a) as it is usually the case for ebullition in lakes (Bastviken et al., 2004; Wik et al., 2013), hydroelectric reservoirs (Galy-Lacaux et al., 1999; Keller and Stallard, 1994), estuaries (Chanton et al., 1989) and marine environment (Algar and Boudreau, 2010; Martens and Val Klump, 1980). According to our data set, emission can be enhanced by a factor of 5 for a water depth difference of 10 m which corresponds to the observed maximum seasonal water level variations at NT2. Though measured in different seasons, diffusive fluxes measured by FC in the EC footprint are

BGD
11, 3271–3317, 2014

constant for the four deployments (see Table 1). This implies that seasonal variation of the CH_4 emissions at a single site is mostly controlled by water level differences and subsequent ebullition. However, this does not exclude that CH_4 emissions are higher during the warm dry season than during cooler seasons as a consequence of enhanced methanogenesis with higher temperature (Duc at al., 2010). It appears that the effect of water level change (6–9 cm), is proportionally stronger in shallow water (2 m) than in deep water (10.5 m) (June 2011, Fig. 3b), meaning that the same water level change could favor higher fluxes in shallow area than in deep waters. This effect is well describes with the specific water level change (Fig. 3c): fluxes were lower when daily variations of the depth were 5 to 7 cm, corresponding to specific water level changes of less than 1 % for most of the field campaigns (March 2010 and 2011), than in June 2011 when the same water level variations corresponded to a specific water level change of 4–5 % which triggered emissions up to 100 mmol m^{-2} d^{-1}. Overall, in the context of this subtropical hydroelectric reservoir with a high contribution of ebullition, these results show that the hydrostatic pressure plays an important role in controlling the CH_4 fluxes since (1) the water depth explains about 70 % (Fig. 3a) of the variability of the CH_4 emissions, (2) seasonal variations of CH_4 emissions by a factor of 5 are mostly due to the enhancement of ebullition due to the low water level in the WD season and, (3) the effect of change in water level on ebullition is more effective in shallow area than in deeper zone of aquatic ecosystems.

4.3 Effect of atmospheric pressure on diurnal cycle of total CH_4 emissions (DE_{EC})

During the analysis of the DE_{EC} time series (Fig. S1), it appeared that two CH_4 peaks of emissions were occurring daily. In order to investigate the drivers of these enhanced emissions, DE_{EC} flux data were binned by time of the day and then averaged for each deployment. A clear diurnal bimodal pattern of DE_{EC} fluxes, with a first peak in the middle of the night (between midnight and 3.00 a.m.) and a second one around noon was observed during all four campaigns (Fig. 4a–d), and is apparently related to the

BGD
11, 3271–3317, 2014

semidiurnal evolution of the atmospheric pressure (a phenomenon due to global atmospheric tides). Diurnal pattern of CH_4 emissions was also recently evidenced by Sahlée et al. (2014) who measured CH_4 fluxes using a EC system over a natural lake in Sweden. They observed higher fluxes at nighttime linked to enhanced diffusion through convective mixing (McIntyre et al., 2010; Sahlée et al., 2014). At NT2, 30 mn-binned DE_{EC} is anti-correlated with atmospheric pressure (Fig. 4a–d). Furthermore, DE_{EC} was found to be anti-correlated with change in atmospheric pressure in every 30 mn (Fig. 4e–h), evidencing a strong control of the atmospheric pressure change over the fluxes, most likely through ebullition (Fig. 4e–h). It is noteworthy to point out that the coefficient of determination is better for the campaign with the lower water depth at the EC site (1.5 m, June 2011, Fig. 4e–h) evidencing that the variations of the atmospheric pressure have more effect at low hydrostatic pressure (higher relative change in pressure). We also calculated buoyancy fluxes in order to look for the potential occurrence of high diffusive fluxes due to convective mixing (Fig. 4i–k) as in McIntyre et al. (2010) and Sahlée et al. (2014). On one hand, nighttime peak of CH_4 emissions coincides with both the constant and low buoyancy fluxes (i.e.; most instable water column), and moderate pressure drop. On the other hand, daytime peak of CH_4 emissions are linked with maximum buoyancy fluxes (i.e. most stable water column). Both observation tend to prove that CH_4 bursts in the night and around noon (up to 100 mmol m^{-2} d^{-1}) could be entirely attributed to the atmospheric pressure drops that triggered ebullition, more than any buoyancy effect (constant during the night, not present during the day).

The effect of pressure on ebullition was already shown in natural lakes (Casper et al., 2000; Eugster et al., 2011; Mattson and Lickens, 1990; Wik et al., 2013) and peatlands (Fechner-Levy and Hemond, 1996; Tokida et al., 2005), and the effect of buoyancy fluxes on diffusive fluxes in lakes (McIntyre et al., 2010; Sahlée et al., 2014), but this is the first time that a daily bimodal variation of CH_4 emissions is evidenced. CH_4 emissions around noon were approximately 10 times as high as fluxes near sunset and sunrise (Fig. 4l–o) and 2 times higher than during the nighttime for all EC deployments ($p = 0.0036$, $p = 0.0002$, $p = 0.0015$ and $p < 0.0001$ respectively for May 2009,

BGD
11, 3271–3317, 2014

March 2010, March 2011 and June 2011, Mann–Whitney test). This implies that the quantification of CH_4 emissions by ebullition and diffusion from inland aquatic ecosystems has to be done over 24 h cycles in order to obtain realistic estimates.

4.4 Temporal and spatial variations of CH_4 ebullition (E_{FUN})

By definition, EC systems are not suitable for the exploration of fine spatial variations and of effect of water depth on ebullition within a single season. Because of logistic difficulties, it was not possible to leave the EC system on site for a full year. As a matter of consequence, we also deployed submerged funnels at 44 locations spread over seven stations. Stations were located in various parts of the reservoir covering different flooded ecosystems, different depths (from 0.4 m to 16 m) being covered in each station. A total of 4811 E_{FUN} measurements were performed in order to characterize the distributions of the volume of gas emitted (V_{EB}, mL $m^{-2} d^{-1}$), bubble CH_4 concentrations and CH_4 ebullition (E_{FUN}). The objective was to explore the spatial and temporal variability of ebullition, and to identify its controlling factors.

The volume of gas emitted V_{EB} averaged 1205 mL $m^{-2} d^{-1}$ and ranged from 0–17 587 mL $m^{-2} d^{-1}$. The positively skewed hyperbolic secant distributions (α = 782.41 and μ = 1205; Fig. 5a) of V_{EB} showed that for most of the records of ebullition (~ 97 %), V_{EB} was below 2000 mL $m^{-2} d^{-1}$. The V_{EB} in the WW season (median = 732 mL $m^{-2} d^{-1}$) was statistically different ($p < 0.0001$, Kruskal Wallis test) and almost two times lower than in the WD (median = 1330 mL $m^{-2} d^{-1}$) and CD (median = 1254 mL $m^{-2} d^{-1}$) seasons.

CH_4 concentration in the bubbles ranged from 0.001 to 69.2 % and was most of the time lower than 30 % (Fig. 5b). The average concentration was 14.9 % that is two to sixfold lower than the concentrations reported for subarctic lakes (34.8 ± 25.2 %, Wik et al., 2013), Siberian thermokarst lakes (82 ± 7 %, Walter et al., 2008), open water and vegetated sites in a beaver pond (47.2 ± 20.8 % and 26.6 ± 12.4 %; Dove et al., 1999) and tropical reservoir (59–66 %, DelSontro et al., 2010). The statistical test ($p < 0.0001$,

BGD
11, 3271–3317, 2014

Kruskal Wallis test) suggested that the CH_4 concentrations in bubbles differed significantly seasonally with CH_4 concentrations 3–5 times higher during the WD season (19.27 ± 12.43 %) than during the WW (7.30 ± 8.78 %) and CD (4.57 ± 5.78 %) seasons. This seasonal variation could be explained by a complex combination of the effect of temperature on both the solubility of CH_4 in water (Yamamoto et al., 1976) and the methanogenesis (Duc et al., 2010), and a potential impact of aerobic CH_4 oxidation on the bubble gas composition. In the WD and WW seasons, bottom water temperatures are similar, but the water column is better oxygenated in the WW season. The lowest CH_4 concentrations in bubbles collected in the WW than in the WD season could be explained by the occurrence of aerobic CH_4 oxidation either in surface sediments before the bubble were released, or in the water column once the bubbles are released. The lowest concentrations during the CD season might result from an increase of (1) the solubility of CH_4 due to 5 °C colder water column temperature than during the other seasons, and (2) potential aerobic oxidation of the CH_4 transported in bubbles since oxygenation of the water column is enhanced by frequent lake overturns (Chanudet et al., 2012). The bubble CH_4 concentration in the WD season ranged from 0.001 to 49 % and was similar whatever the depth of the water column ($p = 0.08$, Kruskal Wallis test), whereas bubble CH_4 concentrations differed among depth zones in WD and CD seasons ($p < 0.0001$ (WD) and $p = 0.0054$ (CD)). In WD season, the bubble CH_4 concentration was two times higher in the shallowest (median = 21.52 %) than in the deepest zones (12.78 %). The decrease in the CH_4 concentration with the water depth can be explained by the dissolution of CH_4 from the bubbles (McGinnis et al., 2006). Overall, we show that the CH_4 concentration in bubbles vary seasonally and spatially by 5 orders of magnitude at the NT2 Reservoir, evidencing that precise extrapolation of the ebullition must take into account both the volume of gas released by the sediments at high resolution (e.g., DelSontro et al., 2010), but also the high variability of CH_4 concentration in the bubbles.

Like V_{EB} and bubble CH_4 concentrations, E_{FUN} fluxes varied by five orders of magnitude at the NT2 Reservoir, and showed a large variability (coefficient of variation =

BGD
11, 3271–3317, 2014

122 %). However, E_{FUN} distribution shows that 95 % of the ebullition records were below 25 mmol m^{-2} d^{-1} (Fig. 5c). On average, ebullition was 8.5 ± 10.5 mmol m^{-2} d^{-1} and ranged from 0–201.7 mmol m^{-2} d^{-1}. At NT2, ebullition is in the lower range of ebullition reported for tropical reservoirs (Abril et al., 2005; DelSontro et al., 2011; dos Santos et al., 2006; Galy-Lacaux et al., 1999; Keller and Stallard, 1994). Ebullition was ten times higher in the WD season (median = 7.9 mmol m^{-2} d^{-1}) than in the WW (median = 0.81 mmol m^{-2} d^{-1}) and CD season (median = 1.3 mmol m^{-2} d^{-1}) (Fig. 6a). This might be related to the dependency of CH_4 solubility and production on temperature, and to the dependency of ebullition on water depth and change in the water depth as explained before. Ebullition from flooded dense forest, degraded forest and agricultural lands was similar during the WW and CD seasons ($p = 0.1077$ (WW) and $p = 0.2324$ (CD), Kruskal Wallis test; Fig. 6b) but slightly lower in the dense forest (median = 6.46 mmol m^{-2} d^{-1}) than in the degraded forests (median = 8.3 mmol m^{-2} d^{-1}) and agricultural lands (8.63 mmol m^{-2} d^{-1}) during the WD season. The ebullition dependency on water depth varies with season (Fig. 6c). Ebullition decreases significantly with depth in the WD season whereas that decrease was not significant for the low emissions of the CD season. This implies that the annual extrapolation of ebullition must account for the seasonal evolution of the ebullition vs. depth relationship.

4.5 Controlling factors on CH_4 ebullition (E_{FUN})

According to our results on short term variation of ebullition obtained from EC and previous works based on both EC and funnels, ebullition fluxes were plotted against water level, water level change, specific water level change, atmospheric pressure, change in atmospheric pressure and bottom temperature. The scatter in different regressions between ebullition and the controlling factors is high probably because ebullition is controlled by a combination of these parameters all together (Fig. 7). Effect of both water depth and the atmospheric pressure were combined by calculating the total static pressure (TSP) and the change in TSP in mH_2O at the bottom of the reservoir, which is the sum of atmospheric and hydrostatic pressure changes. These two parameters

BGD
11, 3271–3317, 2014

were then correlated with ebullition using an exponential decrease regression model (Fig. 7f and g).

Ebullition decreased from 203 to 0 mmol m^{-2} d^{-1} for water depth ranging from 0.4 to 16 m (Fig. 7a). The median of all fluxes measured at shallow sites (0.4–3 m: 6.3 mmol m^{-2} d^{-1}) was almost twofold higher than the median in the deepest zone (6–16 m: 2.9 mmol m^{-2} d^{-1}). The correlation between depth and ebullition is highly significant ($p < 0.0001$), but still, this parameter alone only explains 4 % of the variation of the ebullition ($r^2 = 0.04$; Fig. 7a). The dependency of ebullition on the depth could be attributed to two physical processes. First, the deeper the water column is, the higher the hydrostatic pressure is, preventing from the formation of bubbles by increasing the CH_4 solubility in the sediment pore waters. Second, while the CH_4 bubbles escape the sediment, bubbles partly dissolve in the water on their way up to the atmosphere (DelSontro et al., 2010; McGinnis et al., 2006). The percentage of CH_4 dissolution and thereby oxidation increase with the water depth. On the opposite, shallow zones favor bubble formation because they are generally warmer which both stimulates methanogenesis (Duc et al., 2010) and makes CH_4 less soluble (Yamamoto et al., 1976).

As seen above, water depth has an impact on ebullition, but it appears that water depth change (or hydrostatic pressure change) has a stronger effect ($r^2 = 0.23$) on this phenomenon. Water depth and hydrostatic pressure decrease trigger ebullition as demonstrated here (Fig. 7b), in previous works in marine and estuarine environments, and in freshwater wetlands (Boles et al., 2001; Chanton et al., 1989; Engle and Melack, 2000; Martens and Klump, 1980). During the periods of falling water level, ebullition was fivefold higher (median = 7.5 mmol m^{-2} d^{-1}) than the ebullition during increasing water level (median = 1.5 mmol m^{-2} d^{-1}). The correlation shows that the change in the water level alone explains 23 % of the ebullition variability and it evidences why ebullition is significantly higher during the WD season when the water level is falling (negative water level change) than during the WW season when the water level is rising or during the CD season when the water level is stable. The effect of the specific water level change on ebullition (Fig. 7c) is not as high as expected ($p < 0.0001$, $r^2 = 0.13$) on this

BGD
11, 3271–3317, 2014

large dataset of funnel measurements encompassing a wider range of environmental conditions and flooded ecosystems compared to what we obtained with the EC-derived data only. However, for a given water depth, water depth change and specific water level change, ebullition was in the same range whatever it was obtained from EC or funnels. We hypothesize that EC installed in a zone with a very homogeneous land cover (corresponding to flooded agricultural lands) and covering a large footprint allows to better characterize the controlling factors than discrete sampling with funnels over a few cm^2 in various type of flooded ecosystems.

The relationship of ebullition obtained with funnels over 24 h vs. atmospheric pressure and pressure change were highly significant (Fig. 7d and e) but with very low determination coefficients. These much lower r^2 values compared to the one obtained from the EC could be explained by the fact that mean atmospheric pressure change from one day to the other is smaller than the diurnal variations of atmospheric pressure that we observed during the EC deployments.

The magnitude of the atmospheric pressure varied within a small range (9.55–9.70 hPa, or an equivalent of 0.15 m H_2O). As a matter of consequences, our attempt to combine the effect of hydrostatic and atmospheric pressure (i.e. the so-called Total Static Pressure or TSP) was not highly convincing since we did not improve the correlation coefficient using the TSP (Fig. 7f and g) compared to what we observed for the hydrostatic pressure alone.

Finally, the correlation between ebullition and reservoir bottom temperature was unexpected (significant correlation $r^2 = 0.03$, Fig. 7h). Indeed, ebullition was found to be slightly negatively correlated to the temperature. This is contradictory with the fact that high temperature should enhance ebullition by decreasing the CH_4 solubility (Yamamoto et al., 1976) and by enhancing CH_4 production (Conrad, 1989; Duc et al., 2010) as previously stated. The absence of logical correlation between temperature and ebullition is mostly due to the fact that the highest bottom water temperatures were often synchronized with the beginning of the WW season when the ebullition is moderated by the water level increase.Bottom temperature is known to be an important

BGD
11, 3271–3317, 2014

parameter usually influencing biological activity and therefore ebullition, and should be kept as relevant parameter even with low correlation in our case of study. This illustrates the complexity of controlling factors interacting at the same time, and one with each other in a non linear way. As a matter of fact, it is worth trying a non linear method to represent ebullition through several relevant parameters, identified in this section but not necessarily highly correlated with ebullition.

4.6 Extrapolation of ebullition at the NT2 Reservoir scale by ANN

The extrapolation of ebullition from field measurements to the whole NT2 aquatic ecosystems is challenging. In all studies published so far, the average ebullition is multiplied by the surface area of the shallow zone where ebullition was measured (e.g., Abril et al., 2005; Wik et al., 2013), by type of habitat (e.g., Smith et al., 2000) or by a combination of the two approaches (DelSontro et al., 2011). Our dataset together with the determination of some major controlling factors of ebullition allowed us an attempt for the first time of the extrapolation of this major CH_4 pathway based on physical processes.

As a first approach we used multi linear regressions (MLR). We obtained good correlations with the change in the total static pressure. However, we were able to explain only 21 % of the variance of the ebullition fluxes. The relatively low percentage of explained variance revealed that the complexity of the interactions between the controlling factors of the ebullition is only partially resolved through simple linear equations. A non-linear approach was used to model ebullition fluxes using an ANN. Taking into account controlling factors integrators of several parameters, enhanced in the previous section (total static pressure, change in total static pressure) and reservoir bottom temperature, resulted in a much better agreement between calculated and measured ebullition fluxes ($r^2 = 0.46$, $p < 0.0001$; Fig. S3). Indeed, a step by step study with the ANN revealed that the non linear equation with one input parameter (Total change in TSP) gives an $r^2 = 0.26$. 2 input parameters (Total change in TSP and TSP) gives $r^2 = 0.39$. The addition of bottom temperature leads to the best result of $r^2 = 0.46$. The daily time series

BGD
11, 3271–3317, 2014

of the bottom reservoir temperature and atmospheric pressure are shown in Fig. 8a, and the estimated area-weighted modeled ebullition fluxes together with the measurements at the NT2 Reservoir from January 2009 till August 2013 are shown on Fig. 8b. Over the span of this study, ebullition remained unexpectedly constant whereas total emissions from hydroelectric reservoirs are known to decrease with time (Abril et al., 2005; Barros et al., 2011) due to the exhaustion of the source of organic matter fueling the emissions. The modeled ebullition flux (Fig. 8b) exhibits large seasonal peaks ($25.9 \pm 9.3\,\mathrm{mmol\,m^{-2}\,d^{-1}}$) at the transition between the CD and WD seasons. The peaks are anti-correlated with the water level variations (Fig. 8b), and occur during the periods when both atmospheric pressure is decreasing and water temperature increasing. Due to the high seasonal variations, 50 % of the CH_4 emitted by the NT2 Reservoir each year is released within 4 months even if this period corresponds to the lowest surface of the reservoir. On a yearly basis, ebullition would represent 60–80 % of total emissions (diffusion and ebullition) at the surface of the NT2 Reservoir. This underlines that the estimate of ebullition from an aquatic ecosystem with large water level variations requires high frequency measurements over the period of falling water level since the water level as well as its variations and the concomitant temperature variations have a strong impact on ebullition and ultimately on total emissions.

The ANN model allowed us to simulate the ebullition over a 4 year period by using a few basic meteorological and limnological input data and a one-year intensive monitoring of CH_4 ebullition. This approach constitutes a costless, effortless and powerful gap-filling tool allowing the obtaining of past and future ebullition time series for ecosystems in steady state like natural wetlands and lakes receiving constant amount of organic matter from the watershed and under the influence of constant meteorological forcing. However, in the case of an hydroelectric reservoirs, this approach must be taken with caution and can only be applied during short periods of time when the evolution of ebullition is not significant as it is the case for NT2 during our study or once it reaches its steady state (4–15 years after flooding; Abril et al., 2005; Teodoru et al., 2012).

BGD
11, 3271–3317, 2014

5 Conclusions

Using a set of classical techniques for the discrete measurements of CH_4 diffusive (FC) and ebullition (funnels), and the recently developed EC techniques for the measurement of total CH_4 emissions over large surfaces, we confirmed that the EC system is able to capture continuously and at a 30 min-frequency the two main pathways of CH4 release in inland aquatic ecosystems.

The EC system allowed to evidence a diurnal bimodal pattern of CH_4 emissions following semi-diurnal variation of the atmospheric pressure. Daily atmospheric air pressure drops during all seasons and whatever the depth of the water column, triggers CH_4 ebullition, resulting in a first maximum of CH_4 emissions in the middle of the day. At night, a second and moderate peak of CH_4 emission was recorded due to the combination of a smaller pressure drop and a potential enhancement of the diffusive fluxes because of turbulence generated by heat loss. This might be a common feature in wetlands where the methanogenesis is active enough to induce a storage of CH_4 in the sediments or flooded soils. This diurnal pattern implies that precise estimate of CH_4 emissions from aquatic ecosystems require high frequency measurements over 24 h in order to capture the daily hot moments of emissions that could contribute up to 50 % of daily emissions in a few hours.

We have shown that both the concentration of CH_4 in the bubbles reaching the atmosphere and the volume of bubbles are highly variable. The concentration of CH_4 in bubbles exhibited a high seasonality suggesting that estimate of ebullition cannot be done focusing on the volume of bubbles reaching the atmosphere assuming a predetermined concentration of CH_4 in the bubbles for the whole reservoir and all the seasons.

The statistical analysis with MLR revealed that the ebullition fluxes performed with different methods were mostly dependant on the water level and air pressure variations. The use of these linear regressions did not allow the extrapolation of the flux for the entire reservoir. This is because of the potential non-linearity of the processes and

BGD
11, 3271–3317, 2014

the complexity of the interactions between the controlling factors. Non-linearity was taken into account using an ANN model with total static pressure, change in total static pressure, and bottom temperature as input parameters. ANN model was able to explain 46 % of variation in ebullition CH_4 fluxes, and to perform gap-filling for the ebullition fluxes over a four-year period (2009–2013). Our results clearly showed a very high seasonality with 50 % of the yearly CH_4 ebullition occurs within four months of the WD season although the surface water area of the reservoir is at its minimum during this period. Overall, ebullition contributed 60–80 % of total emissions at the surface of the reservoir (disregarding downstream emissions). Our results on ebullition in this recently flooded reservoir together with the only other results available in tropical hydroelectric reservoirs (Petit Saut Reservoir, French Guiana; Abril et al., 2005; Galy-Lacaux et al., 1997) during the first year after impoundment suggest that ebullition is a major and overlooked pathway in young tropical or subtropical hydroelectric reservoirs.

Supplementary material related to this article is available online at http://www.biogeosciences-discuss.net/11/3271/2014/bgd-11-3271-2014-supplement.pdf.

Acknowledgements. Authors are pleased to express their gratitude to Electricité de France (EDF), Nam Theun 2 Power Company Ltd (NTPC) and Hydro-Québec for funding and contribution to the logistic and all team members of the Aquatic and Environmental Laboratory (AE Lab) for their kind support during field campaigns. CD benefited from a Ph.D. grant by EDF.

References

Abril, G., Guérin, F., Richard, S., Delmas, R., Galy-Lacaux, C., Gosse, P., Tremblay, A., Varfalvy, L., Dos Santos, M. A., and Matvienko, B.: Carbon dioxide and methane emissions and the carbon budget of a 10-year old tropical reservoir (Petit Saut, French Guiana), Global Biogeochem. Cy., 19, GB4007, doi:10.1029/2005GB002457, 2005.

BGD
11, 3271–3317, 2014

Abril, G., Richard, S., and Guérin, F.: In situ measurements of dissolved gases (CO_2 and CH_4) in a wide range of concentrations in a tropical reservoir using an equilibrator, Sci. Total Environ., 354, 246–251, 2006.

Abril, G., Commarieu, M. V., and Guérin, F.: Enhanced methane oxidation in an estuarine turbidity maximum, Limnol. Oceanogr., 52, 470–475, 2007.

Algar, C. K. and Boudreau, B. P.: Stability of bubbles in a linear elastic medium: implications for bubble growth in marine sediments. J. Geophys. Res.-Earth, 115, F03012, doi:10.1029/2009JF001312, 2010.

Angel, R. and Conrad, R.: In situ measurement of methane fluxes and analysis of transcribed particulate methane monooxygenase in desert soils, Environ. Microbiol., 11, 2598–2610, doi:10.1111/j.1462-2920.2009.01984.x, 2009.

Aubinet, M., Grelle, A., Ibrom, A., Rannik, Ü., Moncrieff, J., Foken, T., Kowalski, A. S., Martin, P. H., Berbigier, P., Bernhofer, C., Clement, R., Elbers, J., Granier, A., Grünwald, T., Morgenstern, K., Pilegaard, K., Rebmann, C., Snijders, W., Valentini, R., and Vesala, T.: Estimates of the annual net carbon and water exchange of forests: the EUROFLUX methodology, Adv. Ecol. Res., 30, 113–175, 1999.

Barros, N., Cole, J. J., Tranvik, L. J., Prairie, Y. T., Bastviken, D., del Giorgio, P., Roland, F., and Huszar, V.: Carbon emission from hydroelectric reservoirs linked to reservoir age and latitude, Nat. Geosci., 4, 593–596, 2011

Bastviken, D., Cole, J., Pace, M., and Tranvik, L.: Methane emissions from lakes: dependence of lake characteristics, two regional assessments, and a global estimate, Global Biogeochem. Cy., 18, GB4009, doi:10.1029/2004GB002238, 2004.

Bastviken, D., Santoro, A. L., Marotta, H., Pinho, L. Q., Calheiros, D. F., Crill, P., Enrich-Prast, A.: Methane emissions from Pantanal, South America, during the low water season: toward more comprehensive sampling, Environ. Sci. Technol., 44, 5450–5455, 2010.

Bastviken, D., Tranvik, L. J., Downing, J. A., Crill, P. M., and Enrich-Prast, A.: Freshwater methane emissions offset the continental carbon sink, Science, 331, p. 50, 2011.

Boles, J. R., Clark, J. F., Leifer, I., and Washburn, L.: Temporal variation in natural methane seep rate due to tides, Coal Oil Point area, California, J. Geophys. Res., 106, 27077–27086, doi:10.1029/2000JC000774, 2001.

Borges, A. V., Delille, B., Schiettecatte, L.-S., Gazeau, F., Abril, G., and Frankignoulle, M.: Gas transfer velocities of CO_2 in three European estuaries (Randers Fjord, Scheldt and Thames), Limnol. Oceanogr., 49, 1630–1641, 2004.

BGD
11, 3271–3317, 2014

Casper, P., Maberly, S. C., Hall, G. H., and Finlay, B. J.: Fluxes of methane and carbon dioxide from a small productive lake to the atmosphere, Biogeochemistry, 49, 1–19, 2000.
Chanton, J. P. and Martens, C. S.: Seasonal variations in the isotopic composition and rate of methane bubble flux from a tidal freshwater estuary, Global Biogeochem. Cy., 2, 289–298, 1988.
Chanton, J. P., Martens, C. S., and Kelley, C. A.: Gas transport from methane saturated, tidal freshwater and wetland sediments, Limnol. Oceanogr., 34, 807–819, 1989.
Chanudet, V., Fabre, V., and Kaaij, T.: Application of a three-dimensional hydrodynamic model to the Nam Theun 2 Reservoir Lao PDR, J. Great Lakes Res., 382, 260–269, 2012.
Clement, R.: EdiRe Data Software, v.1.5.0.32; University of Edinburgh, Edinburgh, UK, available at: http://www.geos.ed.ac.uk/abs/research/micromet/EdiRe/ (last access: 12 March 2012), 1999.
Cole, J. J. and Caraco, N. F.: Atmospheric exchange of carbon dioxide in a low-wind oligotrophic lake measured by the addition of SF_6, Limnol. Oceanogr., 43, 647–656, 1998.
Conrad, R.: Control of methane production in terrestrial ecosystems, in: Exchange of Trace Gases between Terrestrial Ecosystems and the Atmosphere, edited by: Andrea, M. O. and Schimel, D. S., J. Wiley & Sons, 39–58, 1989.
Delon, C., Serça, D., Boissard, C., Dupont, R., Dutot, A., Laville, P., De Rosnay, P., and Delmas, R.: Soil NO emissions modelling using artificial neural network, Tellus B, 59, 502–513, 2007.
DelSontro, T., McGinnis, D. F., Sobek, S., Ostrovsky, I., and Wehrli, B.: Extreme Methane Emissions from a Swiss Hydropower Reservoir: Contribution from Bubbling Sediments, Environ. Sci. Technol., 44, 2419–2425, 2010.
DelSontro, T., Kunz, M. J., Kempter, T., Wüest, A., Wehrli, B., and Senn, D. B.: Spatial heterogeneity of methane ebullition in a large tropical reservoir, Environ. Sci. Technol., 45, 9866–9873, 2011.
Demarty, M. and Bastien, J.: GHG emissions from hydroelectric reservoirs in tropical and equatorial regions: review of 20 years of CH_4 emission measurements, Energ. Policy, 39, 4197–4206, 2011.
Descloux, S., Chanudet, V., Poilvé, H., and Grégoire, A.: Co-assessment of biomass and soil organic carbon stocks in a future reservoir area located in Southeast Asia, Environ. Monit. Assess., 173, 723–741, 2011.

BGD
11, 3271–3317, 2014

Dlugokencky, E. J., Bruhwiler, L., White, J. W. C., Emmons, L. K., Novelli, P. C., Montzka, S. A., Masarie, K. A., Lang, P. M., Crotwell, A. M., Miller, J. B., and Gatti, L. V.: Observational constraints on recent increases in the atmospheric CH_4 burden, Geophys. Res. Lett., 36, L18803, doi:10.1029/2009GL039780, 2009.

dos Santos, M. A., Rosa, L. P., Sikar, B., Sikar, E., and dos Santos, E. O.: Gross greenhouse gas fluxes from hydro-power reservoir compared to thermo-power plants, Energ. Policy, 34, 481–488, 2006.

Dove, A., Roulet, N., Crill, P., Chanton, J., and Bourbonniere, R.: Methane dynamics of a northern boreal beaver pond, Ecoscience, 6, 577–586, 1999.

Duc, N. T., Crill, P., and Bastviken, D.: Implications of temperature and sediment characteristics on methane formation and oxidation in lake sediments, Biogeochemistry, 100, 185–196, 2010.

Engle, D. and Melack, J. M.: Methane emissions from an Amazon floodplain lake: enhanced release during episodic mixing and during falling water, Biogeochemistry, 51, 71–90, doi:10.1023/A:1006389124823, 2000.

Eugster, W. and Plüss, P.: A fault-tolerant eddy covariance system for measuring CH_4 fluxes, Agr. Forest Meteorol., 150, 841–851, 2010.

Eugster, W., Kling, G. T., Jonas, J. P., McFadden, A., MacIntyre, S., and Chapin III, F. S.: CO_2 exchange between air and water in an arctic Alaskan and midlatitude Swiss lake: importance of convective mixing. J. Geophys. Res., 108, 4362–4380, doi:10.1029/2002JD002653, 2003.

Eugster, W., DelSontro, T., and Sobek, S.: Eddy covariance flux measurements confirm extreme CH_4 emissions from a Swiss hydropower reservoir and resolve their short-term variability, Biogeosciences, 8, 2815–2831, doi:10.5194/bg-8-2815-2011, 2011.

Fechner-Levy, E. J. and Hemond, H. F.: Trapped methane volume and potential effects on methane ebullition in a northern peatland, Limnol. Oceanogr., 41, 1375–1383, doi:10.4319/lo.1996.41.7.1375, 1996.

Foken, T. and Wichura, B.: Tools for quality assessment of surface based flux measurements, Agr. Forest Meteorol., 78, 83–105, doi:10.1016/0168-1923(95)02248-1, 1996.

Frost, T. and Upstill-Goddard, R. C.: Meteorological controls of gas exchange at a small English lake, Limnol. Oceanogr., 47, 1165–1174, 2002.

Galy-Lacaux, C., Delmas, R., Jambert, C., Dumestre, J. F., Labroue, L., Richard, S., and Gosse, P.: Gaseous emissions and oxygen consumption in hydroelectric dams: a case study in French Guiana, Global Biogeochem. Cy., 11, 471–483, 1997.

BGD
11, 3271–3317, 2014

Galy-Lacaux, C., Delmas, R., Kouadio, G., Richard, S., and Gosse, P.: Long term greenhouse gas emission from a hydroelectric reservoir in tropical forest regions, Global Biogeochem. Cy., 13, 503–517, 1999.

Guérin, F. and Abril, G.: Significance of pelagic aerobic methane oxidation in the methane and carbon budget of a tropical reservoir, J. Geophys. Res.-Biogeo., 112, G03006, doi:10.1029/2006JG000393, 2007.

Guérin, F., Abril, G., Richard, S., Burban, B., Reynouard, C., Seyler, P., and Delmas, R.: Methane and carbon dioxide emissions from tropical reservoirs: significance of downstream rivers, Geophys. Res. Lett., 33, L21407, doi:10.1029/2006GL027929, 2006.

Guérin, F., Abril, G., Serça, D., Delon, C., Richard, S., Delmas, R., Tremblay, A., and Varfalvy, L.: Gas transfer velocities of CO_2 and CH_4 in a tropical reservoir and its river downstream, J. Marine Syst., 66, 161–172, 2007.

Ho, D. T., Bliven, L. F., Wanninkhof, R., and Schlosser, P.: The effect of rain on air–water gas exchange, Tellus B, 49, 149–158, 1997.

IPCC: Summary for Policymakers. in: Climate Change 2013: The Physical Science Basis, Contribution of Working Group I to the Fifth Assessment Report of the Intergovernmental Panel on Climate Change, edited by: Stocker, T. F., Qin, D., Plattner, G.-K., Tignor, M., Allen, S. K., Boschung, J., Nauels, A., Xia, Y., Bex, V., and Midgley, P. M., Cambridge University Press, Cambridge, UK and New York, NY, USA, 2013.

Jähne, B., Munnich, K. O., Bosinger, R., Dutzi, A., Huber, W., and Libner, P.: On parameters influencing air-water exchange, J. Geophys. Res., 92, 1937–1949, 1987.

Joyce, J. and Jewell, P. W.: Physical Controls on Methane Ebullition from Reservoirs and Lakes, Environ. Eng. Geosci., 9, 167–178, 2003.

Keller, M. and Stallard, R. F.: Methane emission by bubbling from Gatun Lake, Panama, J. Geophys. Res., 99, 8307–8319, 1994.

Kemenes, A., Forsberg, B. R., and Melack, J. M.: Methane release below a tropical hydroelectric dam, Geophys. Res. Lett., 34, L12809, doi:10.1029/2007GL029479, 2007.

Kljun, N., Calanca, P., Rotach, M. W., and Schmid, H. P.: A simple parameterization for flux footprint predictions, Bound.-Lay. Meteorol., 112, 503–523, 2004.

Kremer, J. N., Nixon, S. W., Buckley, B., and Roques, P.: Technical note: conditions for using the floating chamber method to estimate air–water gas exchange, Estuaries, 26, 985–990, 2003a.

BGD
11, 3271–3317, 2014

Kremer, J. N., Reischauer, A., and D'Avanzo, C.: Estuary-specific variation in the air–water gas exchange coefficient for oxygen, Estuaries, 26, 829–836, 2003b.
Liss, P. S. and Slater, P. G.: Flux of gases across the air–sea interface, Nature, 233, 327–329, 1974.
Long, K. D., Flanagan, L. B., and Cai, T.: Diurnal and seasonal variation in methane emissions in a northern Canadian peatland measured by eddy covariance, Glob. Change Biol., 16, 2420–2435, 2010.
MacIntyre, S., Romero, J. R., and Kling, G. W.: Spatial-temporal variability in mixed layer deepening and lateral advection in an embayment of Lake Victoria, East Africa, Limnol. Oceanogr., 47, 656–671, doi:10.4319/lo.2002.47.3.0656, 2002.
MacIntyre, S., Jonsson, A., Jansson, M., Aberg, J., Turney, D. E., and Miller, S. D.: Buoyancy flux, turbulence, and the gas transfer coefficient in a stratified lake, Geophys. Res. Lett., 37, L24604, doi:10.1029/2010GL044164, 2010.
Mahrt, L., Sun, J., Blumen, W., Delany, T., and Oncley, S.: Nocturnal boundary-layer regimes, Bound-Lay. Meteorol., 88, 255–278, doi:10.1023/A:1001171313493, 1998.
Martens, C. S. and Klump, J. V.: Biogeochemical cycling in an organic-rich coastal marine basin. 4. An organic carbon budget for sediments dominated by sulfate reduction and methanogenesis, Geochim. Cosmochim. Ac., 48, 1987–2004, 1980.
Matthews, C. J. D., Saint-Louis, V. L., and Hesslein, R. H.: Comparison of three techniques used to measure diffusive gas exchange from sheltered aquatic surfaces, Environ. Sci. Technol., 37, 772–780, 2003.
Mattson, M. D. and Likens, G. E.: Air pressure and methane fluxes, Nature, 347, 718–719, 1990.
McDermitt, D., Burba, G., Xu, L., Anderson, T., Komissarov, A., Riensche, B., Schedlbauer, J., Starr, G., Zona, D., Oechel, W., Oberbauer, S., and Hastings, S.: A new low-power, open-path instrument for measuring methane flux by eddy covariance, Appl. Phys. B 102, 391–405, 2011.
McGinnis, D. F., Greinert, J., Artemov, Y., Beaubien, S. E., and Wüest, A.: The fate of rising methane bubbles in stratified waters: how much methane reaches the atmosphere?, J. Geophys. Res., 111, C09007, doi:10.1029/2005JC003183, 2006.
McNeil, C. and D'Asaro, E.: Parameterization of air–sea gas fluxes at extreme wind speeds, J. Marine Syst., 66, 110–121, 2007.

BGD
11, 3271–3317, 2014

Morrissey, L. A. and Livingston, G. P.: methane emissions from Alaska Arctic tundra: an assessment of local spatial variability, J. Geophys. Res., 97, 16661–16670, doi:10.1029/92JD00063, 1992.
NTPC (Nam Theun 2 Power Company).: Environmental Assessment and Management Plan – Nam Theun 2 Hydroelectric Project, Nam Theun 2 Power Company, Vientiane, Internal report, 212 pp., 2005.
Sahlée, E., Rutgersson, A., Podgrajsek, E., and Bergström, H.: Influence from surrounding land on the turbulence measurements above a lake, Bound.-Lay. Meteorol., 150, 235–258, 2014.
Schubert, C. J., Diem, T., and Eugster, W.: Methane emissions from a small wind shielded lake determined by eddy covariance, flux chambers, anchored funnels, and boundary model calculations: a comparison, Environ. Sci. Technol., 46, 4515–4522, 2012.
Smith, L. K., Lewis, W. M., Chanton, J. P., Cronin, G., and Hamilton. S. K.: Methane emissions from the Orinoco River floodplain, Venezuela, Biogeochemistry, 51, 113–140, 2000.
St. Louis, V. L., Kelly, C. A., Duchemin, E., Rudd, J. W. M., and Rosenberg, D. M.: Reservoir surfaces as sources of greenhouse gases to the atmosphere: a global estimate, Bioscience, 50, 766–775, 2000.
Teodoru, C. R., Bastien, J., Bonneville, M. C., del Giorgio, P. A., Demarty, M., Garneau, M., Hélie, J. F., Pelletier, L., Prairie, Y. T., Roulet, N. T., Strachan, I. B., and Tremblay, A.: The net carbon footprint of a newly-created boreal hydroelectric reservoir, Global Biogeochem. Cy., 26, GB2016, doi:10.1029/2011GB004187, 2012.
Tokida, T., Miyazaki, T., and Mizoguchi, M.: Ebullition of methane from peat with falling atmospheric pressure, Geophys. Res. Lett., 32, L13823, doi:10.1029/2005GL022949, 2005.
Vachon, D., Prairie, Y. T., and Cole, J. J.: The relationship between near-surface turbulence and gas transfer velocity in freshwater systems and its implications for floating chamber measurements of gas exchange, Limnol. Oceanogr., 55, 1723–1732, doi:10.4319/lo.2010.55.4.1723, 2010.
Vapnik, V. N.: The nature of statistical learning theory, Springer, 1995.
Varadharajan, C. and Hemond, H. F.: Time-series analysis of high-resolution ebullition fluxes from a stratified, freshwater lake, J. Geophys. Res.-Biogeo., 117, G02004, doi:10.1029/2011JG001866, 2012.
Varis, O., Kummu, M., Härkönen, S., and Huttunen, J.: Greenhouse gas emissions from reservoirs. in: Impacts of Large Dams: a Global Assessment, edited by: Tortajada, C., Altin-

BGD
11, 3271–3317, 2014

bilek, D., and Biswas, A. K., Springer, Berlin, 69–94, doi:10.1007/978-3-642-23571-9_4, 2012.
Vickers, D. and Mahrt, L.: Quality control and flux sampling problems for tower and aircraft data, J. Atmos. Ocean. Tech., 14, 512–526, doi:10.1175/1520-0426(1997)014<0512:QCAFSP>2.0.CO;2, 1997.
Walter, K. M., Chanton, J. P., Chapin III, F. S., Schuur, E. A. G., and Zimov, S. A.: Methane production and bubble emissions from arctic lakes: isotopic implications for source pathways and ages, J. Geophys. Res., 113, G00A08, doi:10.1029/2007JG000569, 2008.
Wanninkhof, R.: Relationship between gas exchange and wind speed over the ocean, J. Geophys. Res., 97, 7373–7382, 1992.
Wik, M., Crill, P. M., Varner, R. K., and Bastviken, D.: Multiyear measurements of ebullitive methane flux from three subarctic lakes, J. Geophys. Res.-Biogeo., 118, 1307–1321, 2013.
WMO: Guide to Meteorological Instruments and Methods of Observation WMO-No. 8 page I.5–12, 2008.
Yamamoto, S., Alcauskas, J. B., and Crozier, T. E.: Solubility of methane in distilled water and seawater, J. Chem. Eng. Data, 21, 78–80, 1976.

BGD
11, 3271–3317, 2014

Table 1. CH_4 emissions obtained from the different methods. All fluxes are in mmol $m^{-2} d^{-1}$ (average ± standard deviation) and number of measurements (n) given between brackets.

	Method	May-09 Average ± SD (n)	Range	Mar-10 Average ± SD (n)	Range	Mar-11 Average ± SD (n)	Range	Jun-11 Average ± SD (n)	Range	All Average ± SD (n)	Range
Diffusion	D_{GC} [a]	1.2 ± 0.8 (12)	0.2–2.4	0.9 ± 0.5 (9)	0.3–1.8	NA	NA	1.5 (1)	NA	1.1 ± 0.7 (22)	0.2–2.4
	D_{GA} [b]	NA	NA	NA	NA	1.9 ± 1.2 (28)	0.02–5.0	NA	NA	1.9 ± 1.2 (28)	0.02–5.0
	D_{TBL} [c]	1.5 ± 2.2 (14)	0.1–8.9	1.3 ± 0.8 (12)	0.5–3.6	1.1 ± 2.0 (52)	0.07–14.8	1.9 ± 2.5 (19)	0.09–11.2	1.4 ± 2.0 (97)	0.07–14.8
Ebullition	E_{FUN} [d]	1.6 ± 2.9 (9)	0.0–9.9	NA	NA	4.2 ± 3.6 (95)	0.2–21.7	28 ± 11 (126)	10–65	17.1 ± 14.7 (231)	0.0–65.0
	E_{GA} [e]	NA	NA	NA	NA	4.6 ± 7.1 (30)	0–24.6	NA	NA	4.6 ± 7.1 (30)	0–24.6
Total	DE_{GC} [f]	1.9 ± 2.2 (16)	0.2–8.3	8.4 ± 17.4 (24)	0.2–68.8	8.9 ± 10.5 (60)	0.02–49.0	54.0 ± 35.0 (21)	1.4–132.0	15.8 ± 25.2 (121)	0.02–132
	DE_{EC} [g]	6.5 ± 3.3 (39)	2.1–16.1	5.8 ± 5.0 (138)	0.2–26.8	7.2 ± 2.9 (105)	2.8–16.8	29 ± 16 (133)	6.0–103.0	13.6 ± 14.5 (415)	0.2–103

Note: [a] Diffusion by floating chamber (FC) and post-analysis with gas chromatography; [b] diffusion by FC and in situ gas analyzer; [c] diffusion calculated by thin boundary layer (TBL) method from surface CH_4 concentrations; [d] ebullition by submerged funnel; [e] ebullition by FC and in situ gas analyzer; [f] total emissions by FC (diffusion + ebullition) affected by bubbling; [g] emissions measured by eddy covariance.

BGD
11, 3271–3317, 2014

Table 2. Statistical comparisons of different methods to assess CH_4 emissions. All fluxes are in mmol $m^{-2} d^{-1}$ (Average ± standard deviation) and number of measurements (n) given between brackets.

	Diffusion			Diffusion + Ebullition (DE)					
	Method	Average ± SD (n)	test ($p < 0.05$)[1]	Method	Average ± SD (n)	test ($p < 0.05$)[1]	Method	Average ± SD (n)	test ($p < 0.05$)[1]
May-09	D_{GC}	1.2 ± 0.8 (12)	0.6027	DE_{GC}	1.9 ± 2.3 (16)	< 0.0001	DE_{EC}[2]	6.9 ± 2.6 (2)	
	D_{TBL}	1.5 ± 2.2 (14)		DE_{EC}	6.5 ± 3.3 (39)		E_{FUN}[2] + D_{GC}	3.0 ± 1.6 (2)	0.2222
							E_{FUN}[2] + D_{TBL}	3.4 ± 1.7 (2)	0.2533
Mar-10	D_{GC}	0.9 ± 0.5 (9)	0.2815	DE_{GC}	8.4 ± 17.5 (24)	0.0129	DE_{EC}[2]	5.7 ± 3.7 (14)	
	D_{TBL}	1.3 ± 0.8 (12)		DE_{EC}	5.8 ± 5.0 (138)		E_{FUN}[2] + D_{GC}		
							E_{FUN}[2] + D_{TBL}		
Mar-11	D_{GA}	1.9 ± 1.2 (28)	0.0513	DE_{GC}	8.9 ± 10.5 (58)	0.1075	DE_{EC}[2]	7.2 ± 0.8 (4)	
	D_{TBL}	1.1 ± 2.0 (52)		DE_{EC}	7.2 ± 2.9 (105)		E_{FUN}[2] + D_{GA}	6.1 ± 1.2 (4)	0.20
							E_{FUN}[2] + D_{TBL}	5.6 ± 1.2 (4)	0.057
Jun-11				DE_{GC}	54.3 ± 35.0 (21)	< 0.0001	DE_{EC}[2]	26.6 ± 6.7 (5)	
				DE_{EC}	29.1 ± 16.4 (133)		E_{FUN}[2] + D_{TBL}	30.2 ± 5.5 (5)	0.8413

[1] Difference is significant if $p < 0.05$.
[2] n corresponds to the number of days with EC and funnels common deployments.

BGD
11, 3271–3317, 2014

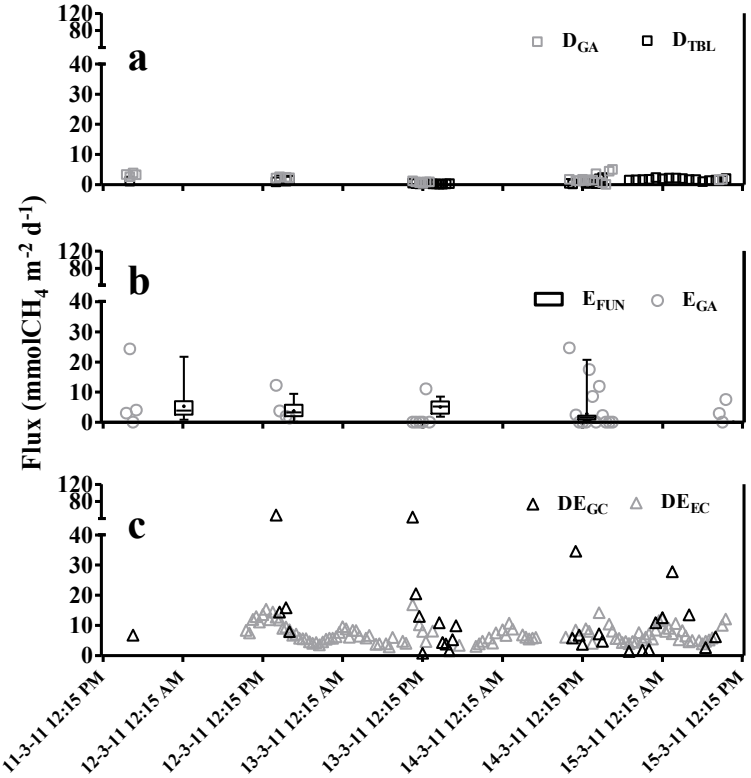

Fig. 1. Time series of **(a)** diffusion, **(b)** ebullition, and **(c)** total (diffusion + ebullition) obtained during March 2011. In **(b)**, boxes show the median ebulliton and the interquartile range, and whiskers denote the full range of all values. Plus sign (+) in the box is showing the mean value. See text for details about different terms in the figure.

BGD
11, 3271–3317, 2014

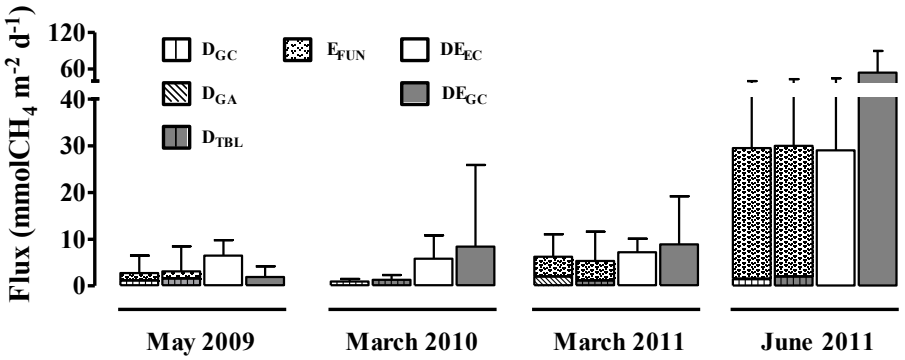

Fig. 2. Inter-comparison of the estimates of CH_4 emissions obtained using the variety of methods deployed during the four field campaigns. See text for details about different terms in the figure.

BGD
11, 3271–3317, 2014

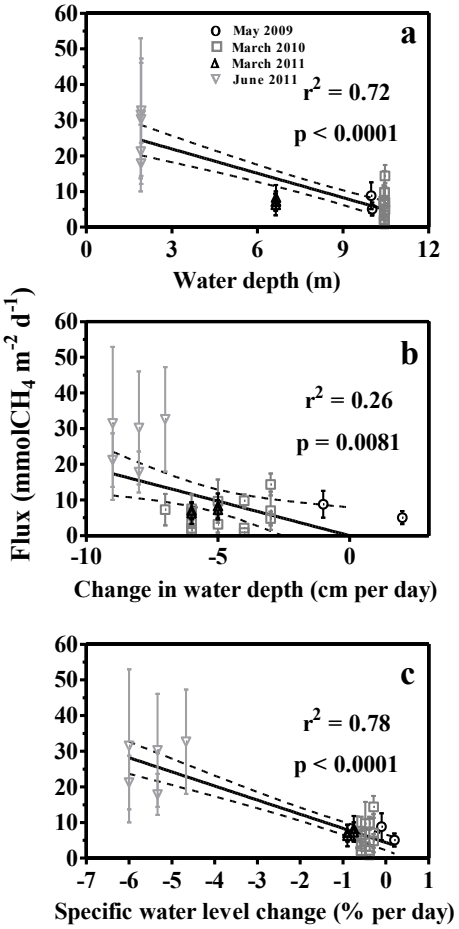

Fig. 3. CH_4 emissions measured by eddy covariance (DE_{EC}) vs. **(a)** water depth, **(b)** change in water depth, and **(c)** specific water level change for the four field campaigns. Note that turbines were not started in May 2009, leading to no water level change during that field campaign.

BGD
11, 3271–3317, 2014

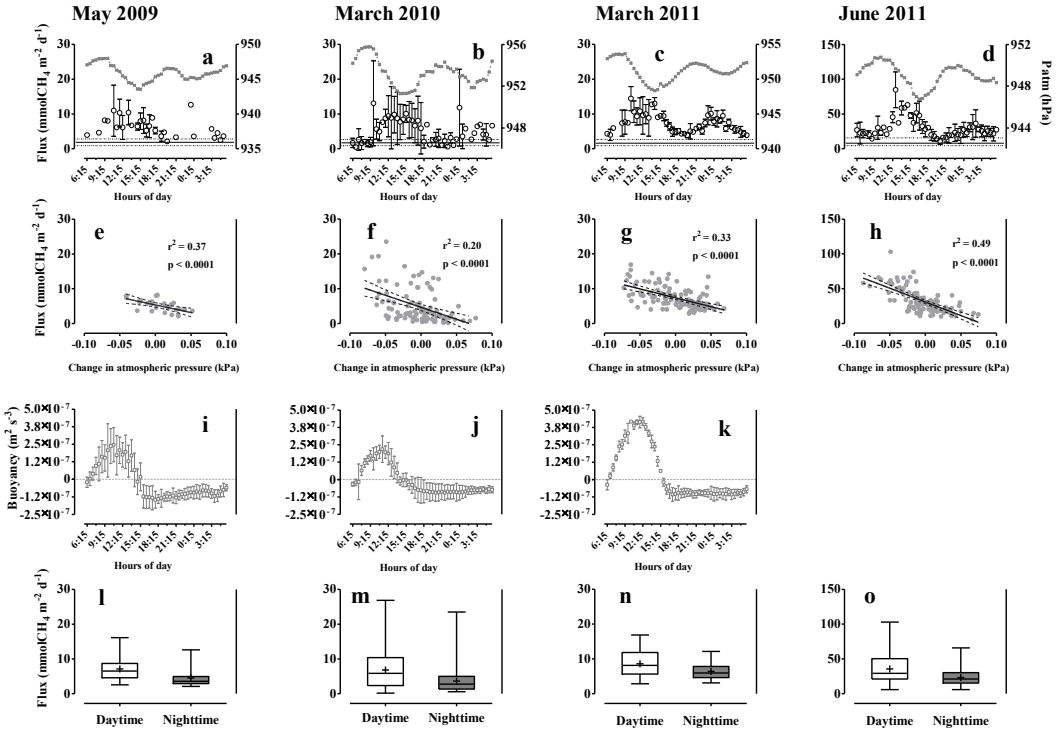

Fig. 4. (a–d) 30 mn-binned CH_4 emissions measured by eddy covariance (DE_{EC}) (circle) and 30 mn-binned atmospheric pressure (cross) for the four field campaigns, **(e–g)**; 30 mn-binned buoyancy flux (note that June 2011 data are not available), **(h–k)** individual 30 min CH_4 emissions measured by eddy covariance (DE_{EC}) vs. change in the atmospheric pressure for the four field campaigns, **(l–o)** night and daytime range for CH_4 emissions measured by eddy covariance (DE_{EC}) for the four field campaigns. Note that y-axis scale differs for the June 2011 campaign **(d, k, o)**.

BGD
11, 3271–3317, 2014

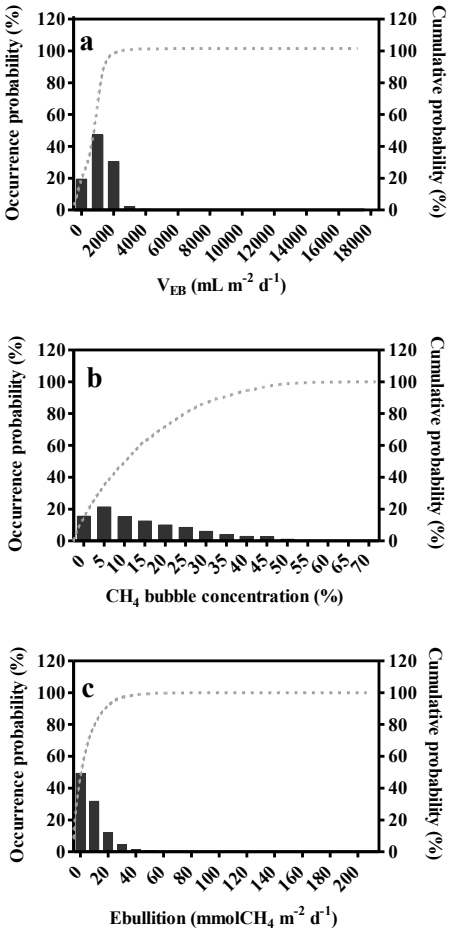

Fig. 5. Histograms showing the distribution of **(a)** ebullition rate, **(b)** CH_4 bubble concentration, and **(c)** ebullition measured by funnels.

BGD
11, 3271–3317, 2014

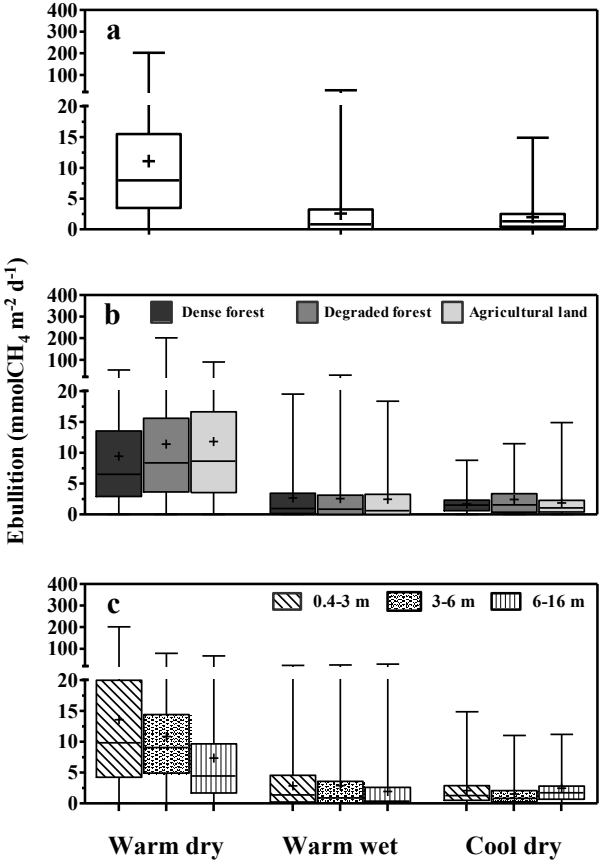

Fig. 6. Ebullition measured by funnels for **(a)** the three different seasons, **(b)** the three major different flooded ecosystems (dense/medium forest, light/degraded forest, and agricultural land), and **(c)** three depth zones.

BGD
11, 3271–3317, 2014

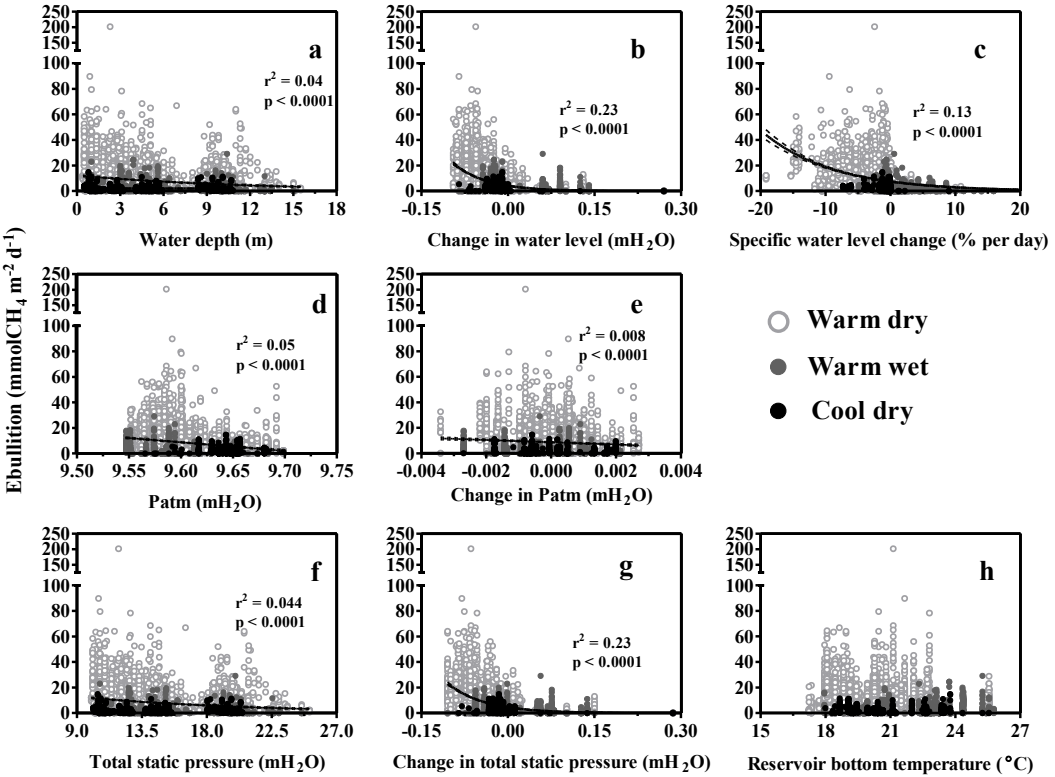

Fig. 7. Ebullition measured by funnels vs. **(a)** water depth, **(b)** change in water level, **(c)** specific water level change, **(d)** atmospheric pressure, **(e)** change in atmospheric pressure, **(f)** total static pressure, **(g)** change in total static pressure, and **(h)** reservoir bottom temperature.

BGD
11, 3271–3317, 2014

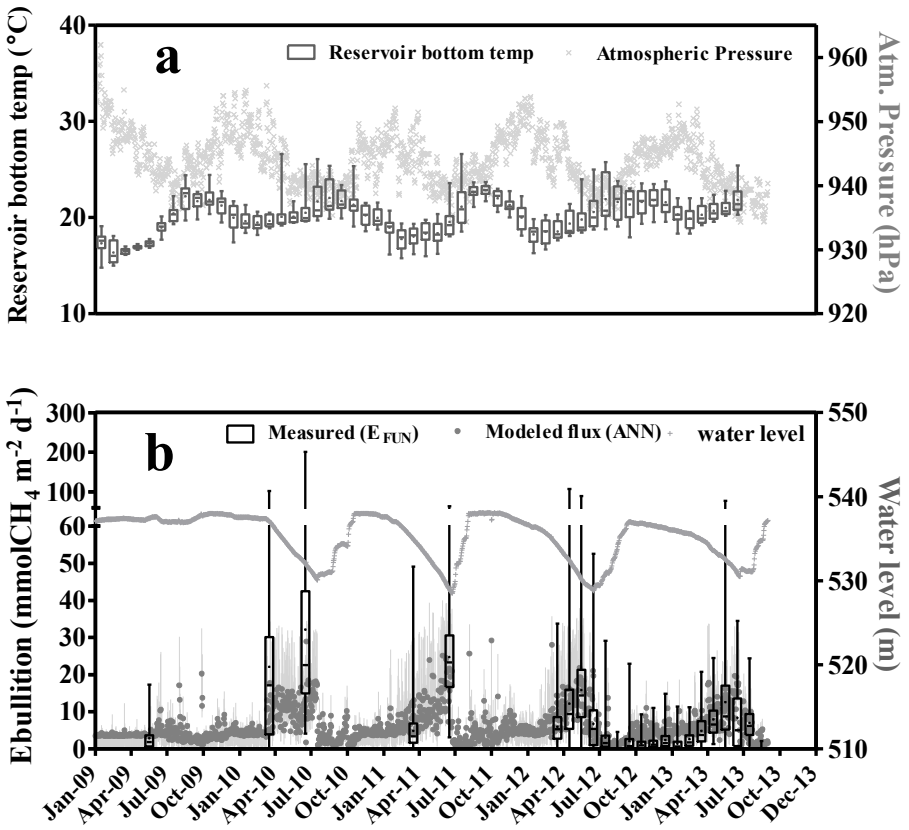

Fig. 8. Time series of the **(a)** reservoir bottom temperature and atmospheric pressure and, **(b)** funnels measured and ANN modeled ebullition fluxes along with reservoir water level. In panel b, boxes show the median concentration and the interquartile range, and whiskers denote the full range of all values. Plus sign (+) in the box is showing the mean value.

BGD
11, 3271–3317, 2014